Diagenesis and Depositional Control in LKU (K, L and M) Formation: A Study to Support Waterflood Activities in Sirikit Oil Field, Thailand.

Kriangkrai Varejaroenchai*

Petroleum Geoscience Program, Department of Geology,
Faculty of Science, Chulalongkorn University, Bangkok 10330, Thailand
*Corresponding author email: Kriangkrai_555@hotmail.com

Abstract

This study focuses on the eastern part of central fault block of the Sirikit Oil Field in the Phitsanulok basin, onshore Thailand. Since 2008 the field has produced mainly crude oil from the early Miocene LKU-K, LKU-L and LKU-M reservoirs which are all deposited in a fluvio-deltaic lacustrine setting. As oil production was starting to decrease, water flood activities were implemented in 2014. However, the results of the water flood revealed that the production performance by water flooding was below expectations. Hence, a number of studies have been undertaken in order to improve the water flood performance. This study is one of them and is focused on the geological factors controlling reservoir performance, especially diagenetic/depositional controls on permeability connections and whether there is pore throat occlusion due to the presence of expansive clays. Until now, the importance of these various factors has not been quantified. The research quantifies these aspects using core from selected intervals and applying petrographic, stable isotope, X-ray powder diffraction (XRD), and glycolation intensity techniques. The latter showed a lack of expansive clays in the studied sediments. Stable isotope values of siderites and ferroan calcites cements illustrates that LKU-K and L reservoir possess more negative $\delta^{18}O$ values than the expected equilibrium compositions of primary calcite-saturated lacustrine waters. The negative shift indicates that the calcite cement which has partially replaced primary aragonite shells was precipitated in an early diagenetic freshwater/meteoric shallow burial environment. The presence of partial preserved aragonitic gastropod Bellamya sp. in the studied cores provides the evidence of a primary freshwater lacustrine setting in the hosting sediments. In contrast to the LKU-K and LKU-L meteoric cement signatures, carbonate cements in the upper LKU-M reservoirs shows more negative $\delta^{13}C$ values indicative of active bacterial aerobic oxidation contributing carbon to bicarbonate in the shallow burial environment. The bicarbonate was formed as an early diagenetic carbonate cement in muddy organic-rich sediment of the LKU-M. In combination these observations indicate that the sands are not connected to an active fluid flow system; otherwise, all the aragonite would be replaced by calcite. In conclusion, the studied core intervals shows evidence of poor connection to a current actively-circulating pore water system. This lack of ongoing connection across many of the thinner sands may help to explain the poor recovery efficiencies in some parts of the field

Keywords: Miocene Sandstone, Water flooding, Fluvio-deltaic lacustrine setting, diagenetic components, Meteoric water, Bacterial aerobic oxidation

1. Introduction

The Sirikit Oil Field is located in the Phitsanulok Basin, about 400 km north of Bangkok. This field is a largest crude oil contributor and it is also the largest Cenozoic rift basin in onshore Thailand, covering an area of about 6,000 km2 (Flint et al., 1988). A string of N-S trending sub-basins constitute the basin (Morley et al., 2007, Pinyo, 2010, Figure 1).

2. Locations and Geological Setting

Morley et al., 2007 summarized the stratigraphy of the Phitsanulok Basin as follows; The earliest stages of the rift (Upper Oligoceane to Lower Miocene) are dominated by coarse immature clastics, deposited as alluvial fans (Sarabop Formation) in an alluvial-plain environment (Khom Fomation) and a fluvial-deltaic to lacustrine environment (Nong Bua Formation). During the Early Miocene, deposition was dominated by lacustrine (Chum Saeng Formation) and fluvio-deltaic (Lan Krabu Formation) conditions. Alternations of these environments juxtaposed fine-grained lacustrine shales (source rocks and seals) with fluvio-deltaic sandstone reservoirs (Figure 2).

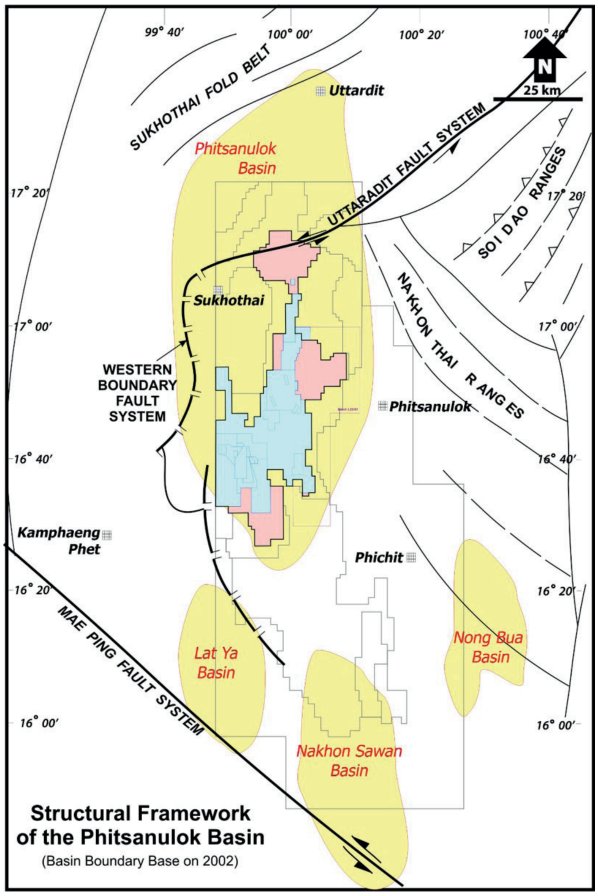

Figure 1. Location of the study area of the Phitsanulok Basin, onshore Thailand. The diagram shows principal structural elements of the Phitsanulok Basin and Central block is shaded green (PTTEP, 2009).

The study area is focused in the eastern part of central block (Figure 3). The main hydrocarbon targets of this area are the LKU-K, LKU-L and LKU-M reservoirs. All reservoir targets were deposited in a fluvio-deltaic environment and have produced crude oil since 2008. As oil production was starting to decrease, water flood activities were implemented in 2014. However, the results of the water flood revealed that the production performance by water flooding was below expectations. Hence, a number of studies have been undertaken in order to improve the water flood performance. One of them is geological quantification of the many postulated root-causes for the poor performance. Suggested geological factors include diagenesis/depositional controls to permeability connections and pore throat occlusion due to the presence of expansive clays. Therefore, this research aims to quantify the importance of these factors in order to understand why the water flood is not working in the way it was first planned.

3. Methodology

The main producing reservoirs of Sirikit oil field in Phitsanulok basin are laminated fluvio-deltaic sandstones of Lan Krabu Formation (K, L, M and P reservoirs). The study area is focused in the eastern part of central block with LKU-K, LKU-L and LKU-M reservoir targets, which have recorded poor water flood performances. Therefore, this study will apply new methods of isotope analyses tied to texture specific petrography and then integrate these results with existing data. The aim is to better understanding diagenesis- depositional controls on poro-perm connectivity in the area and to quantify the influence (if any) of the expansive clay effects in the reservoir's flowability.

Three core intervals were selected from each LKU K, L and M reservoirs for petrography, XRD and stable isotope analysis (carbon-oxygen isotope covariance) in order to better quantify the diagenetic evolution in the reservoirs. Glycolation of clays is a new method for this area and used to analyse the possible presence of expansive clays in the water flooded LKU-K and L reservoirs. Moreover, existing data, such as standard petrography, XRD and SEM have already been performed in parts of the LKU-K sandstones in other wells (Figure 4). These older results are integrated with results from the current study to better inform our current understanding of depositional setting and the intensity of diagenesis alteration.

4. Results and Discussion

4.1 Petrographic study

Four thin sections for petrographic study are tied to lithologies observed in the LKU-K and L reservoirs (shell-rich layers in muddy sandstones). Samples were taken from wells Z03 and Z02 respectively.

The sample (1616.9 m in LKU-K) is dominated by gastropod shells with some bivalve debris. Interestingly, the black coloration of the

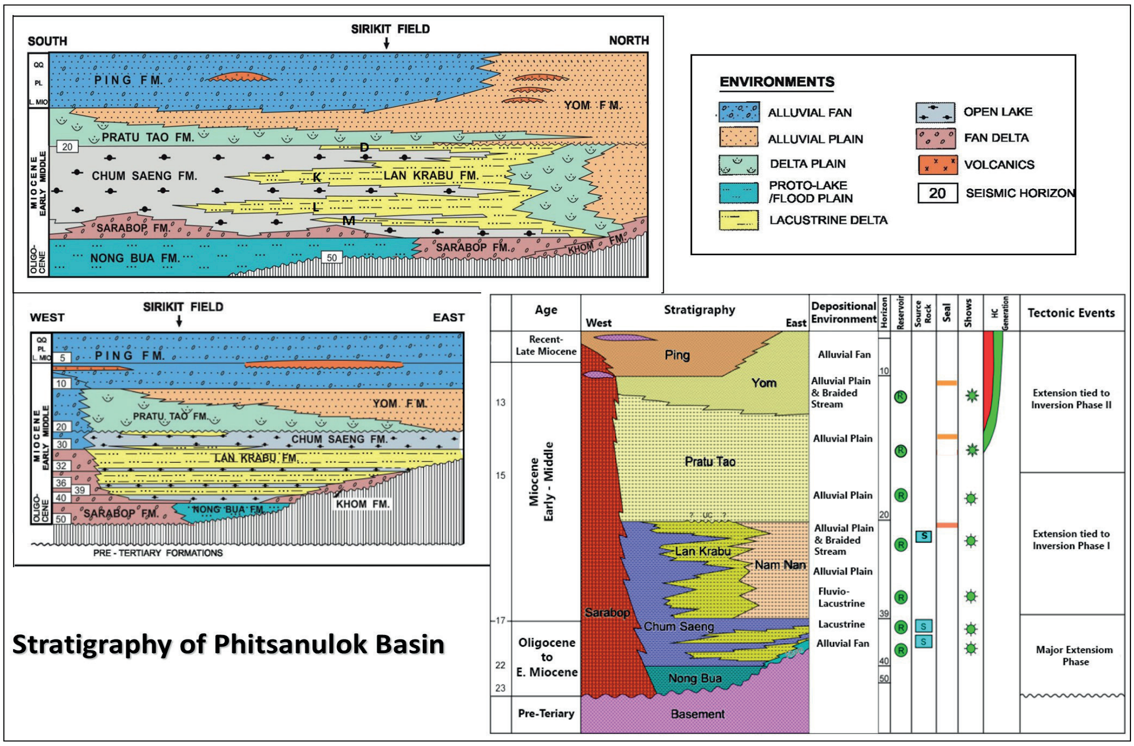

Figure 2 Detailed schematic stratigraphy of the reservoir section, the Lan Krabu Formation prograded from the north into muddy lacustrine conditions pf the Chum Saeng Fm.(Morley, 2007). The lower diagram illustrates the stratigraphic column and the petroleum system elements of the Phitsanulok basin (PTTEP, 2009).

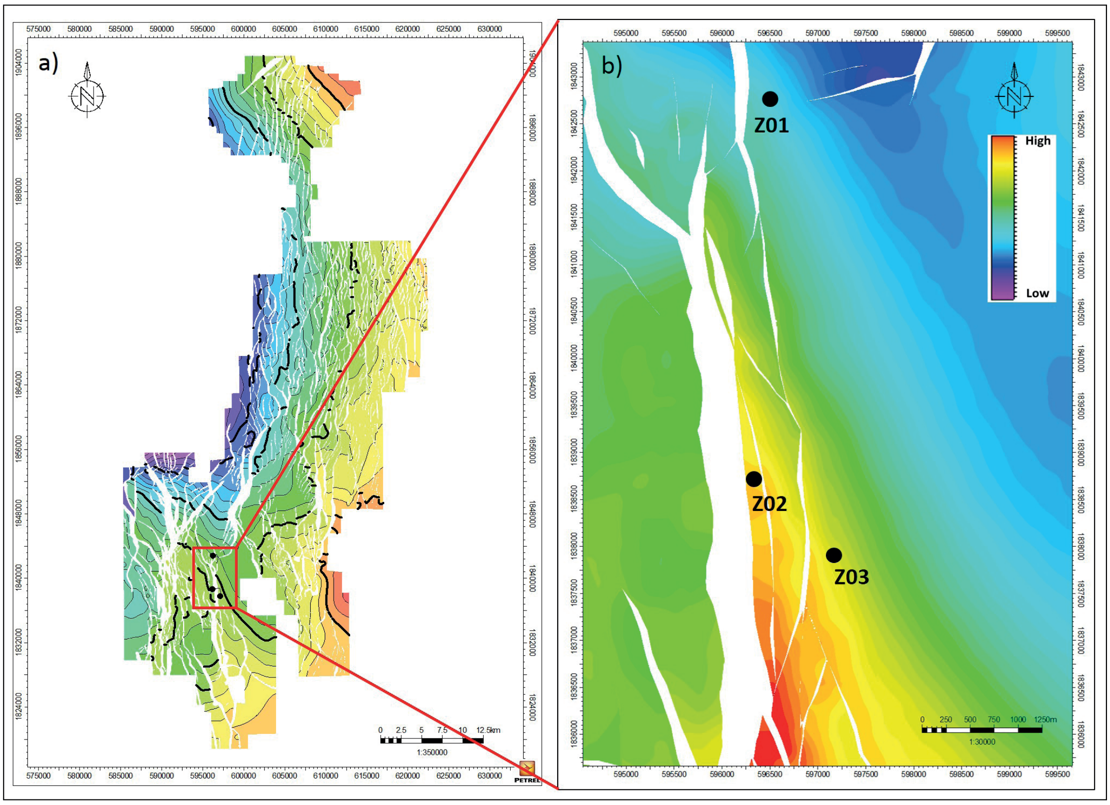

Figure 3 a) Location of the study area outline by Sirikit oil field concession with darker color indicate greater depth and b) the position of the three cored wells under study from the eastern part of central block

Whole rock XRD

Depth(m)	Illite/Smectite	Illite+Mica	Kaolinite	Chlorite	Quartz	K Feldspar	Plagioclase	Calcite	Aragonite	Dolomite	Siderite	Pyrite	Total
1617.04	0.0	TR	TR	0.0	8.9	0.0	0.0	35.5	55.6	0.0	0.0	0.0	100
1617.32	0.0	16.6	2.3	1.2	76.2	2.0	1.6	0.0	0.0	0.0	0.0	0.0	100
1617.46	TR	18.1	2.3	1.3	74.8	1.1	2.4	0.0	0.0	0.0	TR	0.0	100
1617.53	0.6	18.4	2.4	1.2	74.3	1.0	2.1	0.0	0.0	0.0	0.0	0.0	100
1617.97	0.6	18.7	2.2	1.1	68.9	0.9	1.8	5.9	0.0	0.0	TR	0.0	100
1618.11	0.6	16.0	2.3	1.2	70.1	1.0	2.0	6.8	0.0	0.0	0.0	0.0	100
1618.20	TR	14.7	1.1	0.8	79.2	1.4	1.3	1.5	0.0	0.0	TR	0.0	100
1618.26	TR	12.9	1.2	0.6	81.9	1.2	1.5	0.8	0.0	0.0	TR	0.0	100
1618.35	0.0	14.6	1.5	0.7	80.1	1.0	1.4	0.7	0.0	0.0	0.0	0.0	100
1618.42	TR	23.8	2.8	1.3	67.9	0.9	2.4	0.9	0.0	0.0	TR	0.0	100
1620.18	1.3	33.4	4.1	2.1	56.0	1.1	2.0	0.0	0.0	0.0	TR	0.0	100

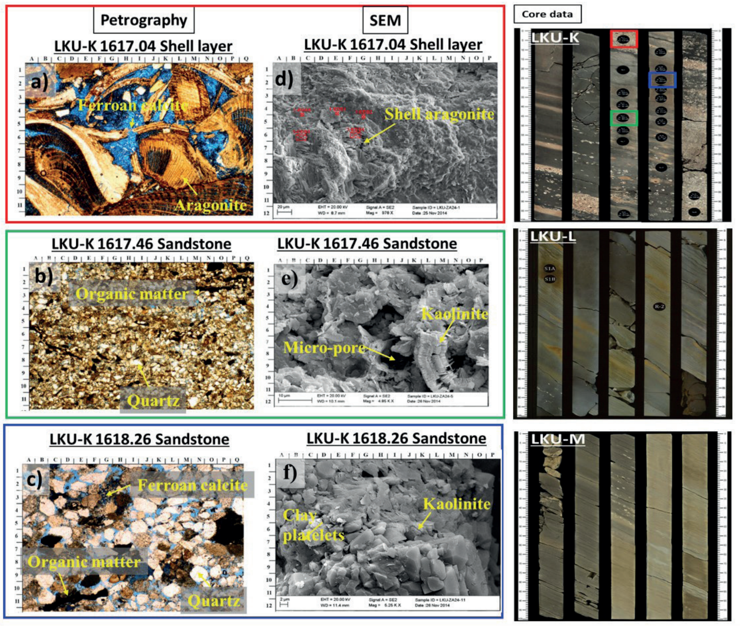

Figure 4 Example of the Petrography, XRD and SEM analyses performed prior to this study in LKU-K sand- stones from an existing well study @ depths of 1617.04, 1617.46 and 1618.26 m. a) Most of this interval comprises calcium carbonate in the form both of aragonite, represented by shell fragments (various shades of yellow and brown in PPL), and calcite, which appears bright-blue when stained, owing to its strongly ferroan nature. b) The sample largely comprises grains of mono- and polycrystalline quartz, which mostly appear clear and white. c) This fine grained sandstone contain a small proportion of ferroan calcite cement. d) This sample comprises a shelly coquina with a ferroan calcite cement, and scattered very-fine grains of quartz and feldspar. The shelly material in places has a fibrous, microporous appearance, where layers of aragonite prisms are separated by layers of calcite cement. e) The sample illustrates a mass of microporous clay particles infilling a pore between sand grains which XRD analysis shows to be the most abundant clay phase. f) Stacks of kaolinite platelets are observed, and the overgrowths appear to include moulds of clay platelets with a kaolinite-like stacked morphology. (Petrography documented as part of internal PTTEP report, Core Plugs Petrographic Analyses, 2015)

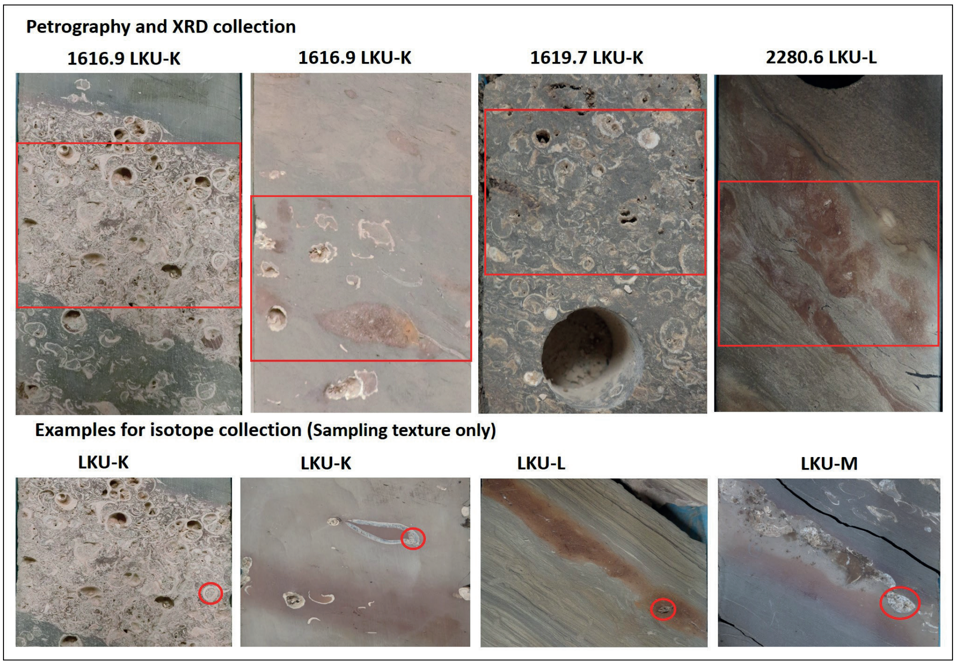

Figure 5 Examples of the sampling approach used in this study for petrography (thin section position indicated by red rectangles) and drill position for isotope and XRD powder were conducted by sampling specific textures collection (indicated by red circles)

Fiegl stained thin section stub shows that there are unreplaced aragonite portions of the shell fragments (shades of brown with prismatic texture). The calcite that has partially replaced the aragonite appears bright yellow-orange, along with cements of sparry ferroan calcite that show a bright blue color in areas stained by potassium ferricyanide (Figure 6a). The alizarin red-S and potassium ferricyanide visible in the lower section of Figure 6b highlights how porosity occurs in these samples and also identifies the current carbonate mineralogy (aragonite/calcite in gastropod/shell fragments show shades of pink orange ,while ferroan calcite appear as blue-dark blue hues).

Clusters of small brown micrite aggregates (< 0.1mm diam) sometimes encased in the cement possibly indicate biogenic features related to periodic (seasonal?) precipitation in the upper water mass of the lake followed by pelagic settling and possible bacterial degradation, (Figure 6c).

Sample No.2 (1617.7m in LKU-K) is very-fine grained sandstone that appear as clear and white cm-scale layers in core. The degree of sorting of detrital grains varies between moderately-to-well sorted and very well-sorted. The dominant grain shape within all samples is typically subangular to subrounded. The aragonite in shell fragments in this sandstone show shades of brown, while siderite/iron oxide appear dark brown to black in thin section (Figure 6d). The aragonite in shell fragments (Shades of brown with prismatic texture) and calcite leaching inside shell show as white to pink colors (Figure 6e).

The sample No.3 (1619.7m in LKU-K) stained with alizarin red-S and potassium ferricyanide is a combination of calcite and aragonite (shades of pink orange), whereas the black stained coloration of thin section stubs indicate aragonite in the unreplaced portions of the shell fragments (shades of brown with prismatic texture) under the Fiegl solution (Ag2SO4+MnSO4). The calcite has partially replaced the aragonite and appears bright yellow-orange in thin section (Figures 6a, 6f). Ferroan calcite cement formed the inside of leaching shells and appears blue in the combined alizarin red-S and potassium ferricyanide stain. (Figure 6g).

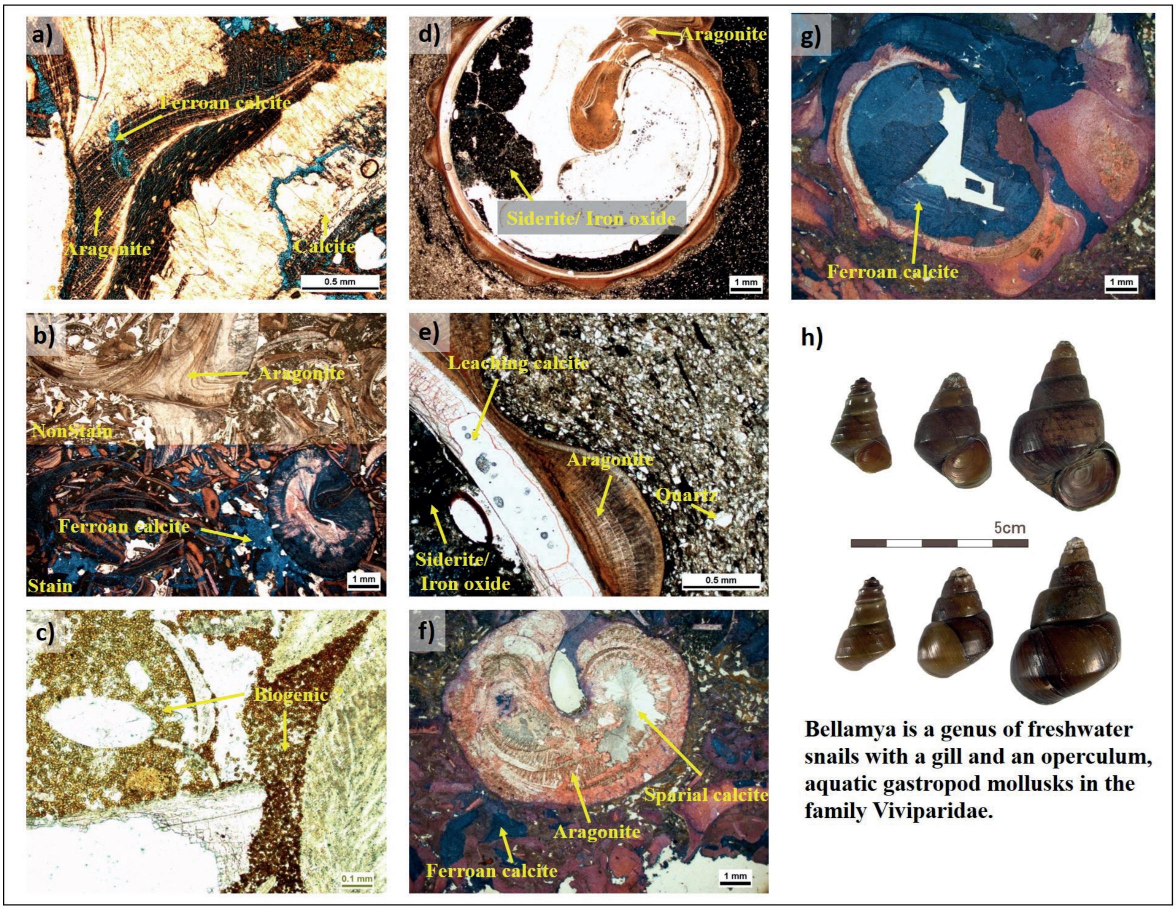

Figure 6 Photomicrographs diagram of LKU-K reservoir with diagenetic mineral from resampling of cores completed during this study to give control in isotope analysis

The sample No.4 (2280.6 m in LKU-L) composes of very-fine grained sandstone appear clear and white. The degree of sorting of the detrital grains hosting the shells is well sorted. The dominant grain shape within all samples is typically sub-angular to angular and interlayered clay showing shades of brown. Micro-fractures (white lineaments) and organic matter smeared along bedding planes were also observed (Figure 7a). Siderite and iron oxide show as brown stains in core. Organic matter, as illustrated in figure 7a and 7b appears opaque in thin section.

4.2 X-ray powder diffraction (XRD)

Six powder samples were analysed in order to identify the minerals in the shell layers, and the dominant mineralogies in the sandstones and clays, as seen in the petrographic study. All samples were selected by drilling specific textures in each cored interval. Results can be divided in to 2 groups as follows:

1) The carbonate group includes calcite, aragonite and ferroan calcite. This mineral association tends to dominate in carbonate layers in the upper LKU-K interval, which makes up much of the overlying siliciclastic section (Lower-Miocene). Samples at 1616.9 m and 1619.7 m in LKU-K (Z03 well) are calcite ($CaCO_3$) dominated, with sub-dominant to trace aragonite ($CaCO_3$) respectively. Note that the whole rock XRD method cannot clearly differentiate calcite and ferroan calcite (whereas stained thin sections can).

2) The siliciclastic group consist of quartz, clay minerals (mostly kaolinite, chlorite) and muscovite. This mineral association is dominant in all sampled sections (LKU-K, -L and –M). Locally , sandstone samples at 1617.7 m in LKU-K (Z03) and 2280.6 m in LKU-L (Z02 well) show siderite ($(Fe,Ca),CO_3$) dominant, with sub-dominant quartz(SiO_2). Siderite is often an early diagenetic precipitate, forming shortly after the host sandstones are deposited (Spiro et al., 1992). Additionally, XRD samples in shale at 1618.8 m in LKU-K (Z03) and 2297.6 m in LKU-L (Z02 well) are muscovite ($KAl_2Si_3AlO_{10}(OH)_2$) dominated and sub-dominated by Chlorite

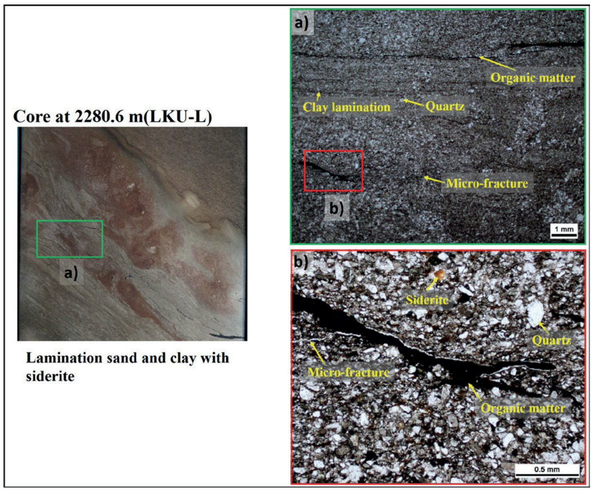

Figure 7 Photomicrograph diagram of LKU-L reservoir with diagenetic minerals from resampling of cores completed during this study to give control in isotope analysis

($(Mg,Al,Fe)_{12}(Si,Al)_8 O_{20}(OH)_{16}$) with a trace of Kaolinite ($Al_2Si_2O_5(OH)_4$).

Traces of kaolinite (Figure 8a) are also seen in SEM images of sandstone at 1617.46 m, which illustrates a mass of microporous clay particles infilling an intergranular pore. Most of the kaolin clays are platy but other clays are typically amorphous, and probably represent slightly altered and partially recrystallized detrital illites.

At 1618.26 m, the sampled fine-grain sandstone is a finely polycrystalline quartzose sediment with grains covered by numerous small overgrowths indicating that some clay is trapped between the overgrowths. This is confirmed at higher-magnifications where stacks of kaolinite platelets are observed, and the overgrowths around position B7 appear to include moulds of clay platelets with a kaolinite-like stacked morphology (Figure 8b).

4.3 Glycolation

Illite-smectite interstratifications are one of the most common clay components of sedimentary rocks and are the most sensitive clay indicators of the degree of diagenesis and low-grade metamorphism. Because of their extremely small grain size, illite / smectite inter- stratifications are easy to concentrate and separate during sedimentation. For these reasons,

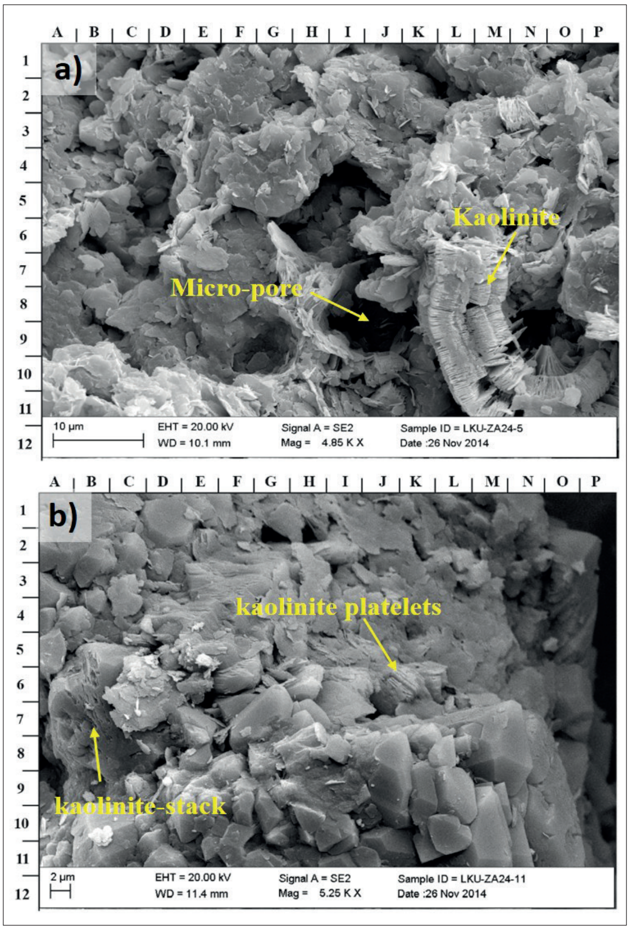

Figure 8 SEM of sandstone at a) 1617.46 and b) 1918.26 m show friable habit kaolinite and kaolinite platelets (booklets).

many clay diagenesis studies concentrate on these minerals (Dunoyer de Segonzac, 1970; Perry and Hower, 1970; Hower et al., 1976; Srodon, 1979).

In the present study, all untreated samples were analyzed by X-ray diffraction to identify the clay minerals present (Table 3). Two samples (Z03 at 1616.18 m and Z02 at 2297.6 m) in shale were glycolated by two methods for clay mineral analysis (Illite / Smectite , Jan Srodoi, 1980):

- Placing the sample in a sealed container with an open dish of glycol

- Making a slurry of the sample and glycol.

Subsequently, X-ray diffractograms were performed and analyzed for both samples. The identification of the individual clay mineral is based on the d-spacing values of their basal reflection as observed on the X-ray diffractograms of untreated sample peak shoulder. When combined with any variation in these d-spacing values in response to glycation the type of clay mineral can be identified.

The results of glycolation in the submitted samples show that only effect of glycolation is to remove a slight "peak shoulder" on the low angle side of the mica peak. It probably indicates that there is "illite with a minor proportion of interlayered smectite in the studied samples Highly water reactive clays were not presented in the submitted samples.

4.4 Stable Isotopes

Stable isotope analysis is used to test the notion of only early stages of diagenesis evaluation being observed in thin sections and X-ray diffraction of shell carbonate layer and sandstone. That is, these samples are known to retain metastable but partially replaced aragonite.

The range of $\delta^{18}O_{PDB}$ is -16.0 % to -6.2 % and the range of $\delta^{13}C_{PDB}$ is -14.8 % to 2.9 % $_{PDB.}$ The carbon – oxygen isotope plot of siderite - and calcite-dominated samples in this study generally shows two largely distinct plot fields on a $\delta^{18}O_{PDB}$ versus $\delta^{13}C_{PDB}$ plot (Figure 9a).

The oxygen isotope compositions indicate that the siderite nodules and layers formed in a freshwater environment, but generally show a range more negative than the expected equilibrium composition (as also discussed in Spiro et al., 1992). The carbon isotope composition may reflect deposition within the bacterial oxidation zones. These particular lacustrine indications allow a detailed study of the isotopic geochemistry of the siderites and an assessment of the geochemical processes leading to their formation in its various forms. This investigation should contribute to a broader understanding of the formation and diagenesis of ferroan carbonates in freshwater organic-rich sediments in Thailand and elsewhere. To my knowledge, this is the first application of the stable isotope technique to the carbonates of Sirikit Oil Field.

Samples with high abundance of siderite have carbon-oxygen plotfields very similar to siderites precipitated in oxygen isotopic equilibrium with modern lake water (Figure 9a compared to 9b). Samples from intervals of low siderite abundance are $\delta^{13}C$ and $\delta^{18}O$ depleted relative to equilibrium with modern lake water. These data suggest that abundant siderite precipitation occurred when the overlying water column was ferruginous (iron meromictic), allowing for enhanced ferrous iron concentrations and dissolved inorganic carbon (DIC) enriched in $\delta^{13}C$ below the chemocline, whereas methanogenesis in waters and sediments influenced by anoxic DIC composition (Wittkop C, 2014).

The carbon isotope composition in synsedimentary and diagenetic carbonates is largely determined by depositional and diagenetic processes in the organic matter and CO_2 exchange with the atmosphere. A schematic presentation of the common diagenetic reactions leads to carbonate deposition and their associated isotopic characteristic is given as Figure 9b. Although small amounts of pyrite do occur, indicative of sulfate reduction processes, these are of very limited importance in a sulfate-poor lacustrine environments, as was likely the case in the study area.

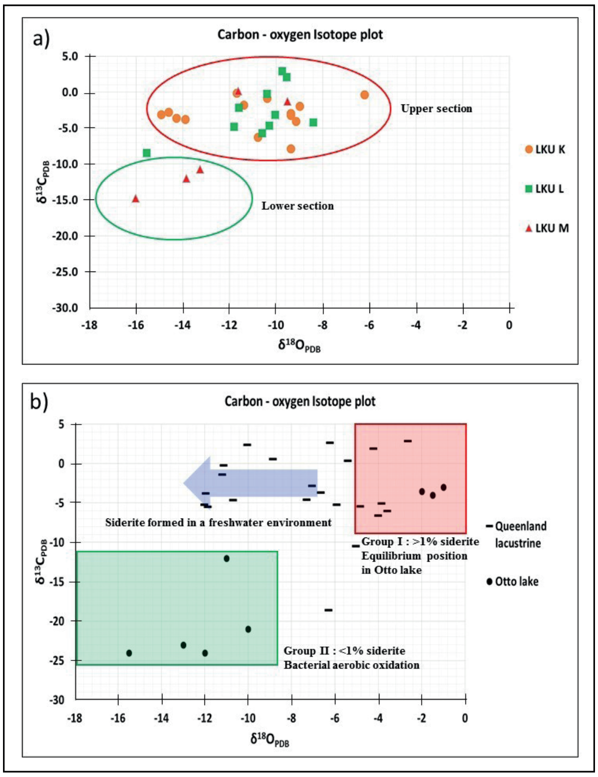

Figure 9 a) $\delta^{13}C$ versus $\delta^{18}O_{PDB}$ plot of the samples in LKU-K, -L and M, separated into 2 groups indicated by red circle for upper and green circle for lower core sections b) Two groupings of siderite precipitates in analogous Tertiary lacustrine sediments from Queensland and Holocene Lake Otto precipitates, both tied to freshwater and bacterial oxidation environments (Gibson, 1992)

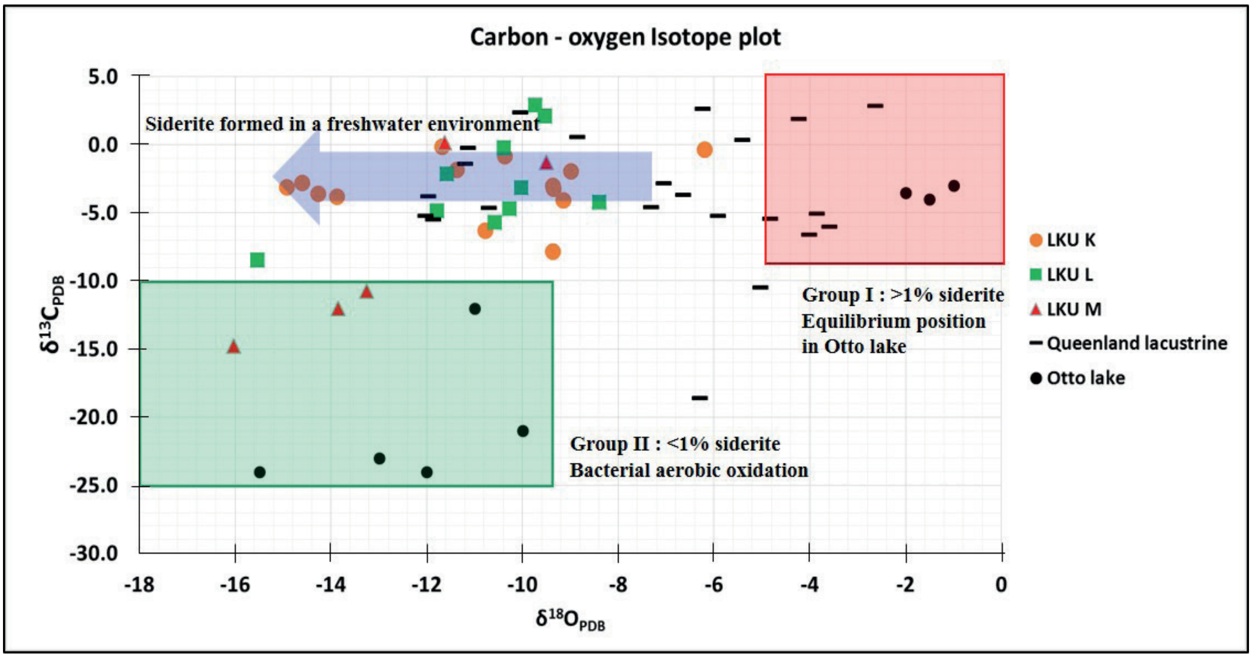

Figure 10 $\delta^{13}C$ versus $\delta^{18}O_{PDB}$ plot overlying results from the study area and from analog siderite settings in freshwater Tertiary lacustrine sediments in Queensland and Holocene Lake

The organic matter has undergone bacterial oxidation and fermentation but it has not reached an advanced thermal maturation stage. Bacterial oxidation would result in the generation of carbonate with light $\delta^{13}C$ values similar to thatof the original organic matter (-25% PDB) while in an anoxic methanogenic zone heavier $\delta^{13}C$ values would be encountered (+ 15%O) (Irwin et al., 1977).

5. Discussion

1) A comparison of the measured set of isotope values in this study, to published carbon- and oxygen-stable isotopic signatures controlled by a combination of methanogenesis, temperature, and water column stratification in Holocene siderite varves (Wittkop, 2014) and eogenetic siderites in Tertiary lacustrine oil shales from Queensland, Australia (Gibson, 1992), shows an impressive overlap of the plot fields (Figure 10).

It seems there is an alignment of data sets between LKU-K, LKU-L (fluvio-deltaic sandstone) isotope fields and published data from fresh water lacustrine regimes. The more negative $\delta^{18}O$ values in the plotfield likely indicate the influence of meteoric water in shallow water burial levels in the fluvio-deltaic section of the recovered cores (indicated by blue arrow in Figure 10).

In contrast, the upper part of LKU-M interval, with isotope values indicated by red triangles in Figure 10, are dominated by muddy lacustrine facies (Tultaveewat, 2015). Levels of organic matter were elevated as these muddy lacustrine sediment accumulated, compared to the sandier higher energy intervals with more oxidation. The latter typified the grainer more marginward depositional setting of sediment in LKU-K and LKU-L units (Figure 11).

Therefore, as this muddy lacustrine sediment was buried, the entrained organics passed through a variety of chemical diagenetic systems such bacterial aerobic oxidation, and anaerobic organic maturation. These alteration systems would have contributed carbon to bicarbonate, which then precipitated as diagenetic carbonate cement in a muddy sediment host in the LKU-M unit.

In carbon- and oxygen-stable isotope plot for the upper LKU-M samples, the $\delta^{13}C$ values sit between 10 – 15% PDB which implies siderite precipitation in a bacterial oxidation system. However, samples from the lower part of LKU-M came from siderites hosted in siltstones, laminated sand lenses and interbeds of sand/mud implying a more open bottom hydrology in what were more permeable sediments compared to those illustrate in Figure 11 so that these values show less negative carbon determination and still reside in the freshwater field.

2) Based on petrography and XRD results. The sandstones and shell layers have been subjected to a similar series of diagenetic processes. These are summarised below:

- Precipitation of Aragonite and calcite in shell fragment
- Partial replacement and leaching of aragonite by calcite (some ferroan)
- Precipitation of siderite
- Formation/modification of clay rims cement
- Grain alteration: formation of authigenic clays and secondary pores
- Illitisation of kaolinite

3) The abundant gastropod fossil in the sampled shell layers is Bellamya sp. This is a genus of freshwater snails , an aquatic gastropod mollusks in the family Viviparidae which is corresponds to the same fossils of Middle Miocene age found in Phetchabun basin (Geology of Phetchabun, DMR, 2009, 1: 50000 map)

4) Illite with a minor proportion of interlayered smectite (from glycolation analysis were aligned with XRD in sandstone as Illite/smectite) is less than 1% (see figure 4).

5) When combined all data can be used to locate of each reservoir facies both depositionally and diagenetically in a fluvio – deltaic – lacustrine depositional model (Figure 11);

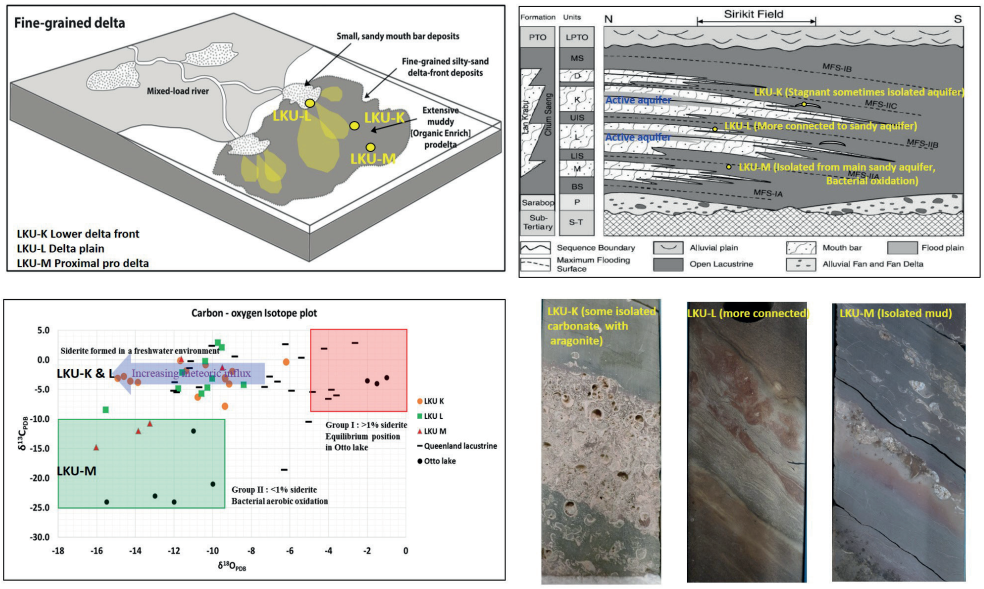

Figure 11 Depositional environment diagram of LKU-K, - L and M after integrated all data (Modified from University of Sargodha, 2007).

- LKU-K reservoir was deposited in lower delta front, as supported by layers of fragmented gastropods indicating periodic high energy deposition in and otherwise muddy setting with ambient fresh water as indicated by the isotope data,
- LKU-L reservoir was deposited in flood plain to shallow lacustrine (delta plain) with floodplain splays in the medial zone with floodplain mudstone and sand sheets (Tultaveewat, 2015) and isotope data show meteoric waters in the pores when early diagenetic siderite was precipitated
- LKU-M reservoir was deposited in more distal deeper water setting dominated by suspended load mud settling and elevated organic levels interbedded with sand lenses isotope data from the siderites indicate a bacterial oxidation system

6. Conclusions

Results of the present study can be used to better understand and improve water flood performance as it shows;

1) Diagenesis is ongoing but slow in this lacustrine delta as aragonite is preserved and isotope analysis indicates siderite values are indicative only of the early stages of diagenesis.

2) Expansive clay minerals are not important controls in the studied cores

3) Sandstones with aragonite shells partially preserved, indicates these sands are not completely connected to an active fluid flow system.

4) Stable isotope values of siderites and ferroan calcites illustrates that LKU-K and L reservoirs possess more negative $\delta^{18}O$ values than the expected equilibrium compositions. The various cements precipitated in a freshwater/ meteoric depositional. Pore water in burial environment were shallow and fresh meteoric waters present at the time the cements formed. The Bellamya sp. (Gastropod) provides fossil evidence of a freshwater depositional environment in the hosting sediment. In contrast the upper LKU-M carbonate cements show more negative $\delta^{13}C$ indicative of a chemical diagenetic systems, such as bacterial aerobic oxidation contributing carbon to bicarbonate which then formed diagenetic carbonate cement in the muddy organic rich sediment in the LKU-M.

5) The Upper part of LKU-M may part of Chum Seang formation, which is potentially be source rock with average TOC about 2.7 % and mostly of type I kerogen.

6) LKU-K core is located in lower delta front, delta plain for LKU-L and pro-delta for LKU-M in a fluvio-deltaic depositional environment.

7) The studied core intervals show evidence of poor connection to a current-actively circulating pore water system.

7. Acknowledgements

I would like to express my gratitude to PTTEP for the opportunity and scholarship to study in the Master Degree of Petroleum Geoscience at Chulalongkorn University and my advisor, Ph.D. Dr. John K. Warren for his full support and expert guidance, recommendations and encouragement throughout my research.

8. References

Dickson, 1966, Carbonate Identification and Genesis as revealed by Staining, J.A.D., Journal of Sedimentary Petrology, Vol. 36, No. 2, p. 491-505.

Flint, S., Stewart, D. J., Hyde, T., Gevers, E.C.A., Dubrule, O. R. F. and Van Riessen, E. D., 1988, Aspects of reservoir geology and production behavior of Sirikit Oil field, Thailand: An integrated study using well and 3-D seismic data, AAPG Bulletin, V. 72, p. 1254 – 1269.

Geology of Phetchabun, DMR, 2009, Bellamya sp., Aquatic gastropod mollusks in the family Viviparidae, P.53, http://www. dmr. go.th/download/digest/Petchabun.pdf

Matha S., 2017, Maturity modeling of the Chum Saeng formation, Phitsanulok basin, Thailand, Published MSc. Thesis, Department of Geology, Chulalongkorn University, p. 44.

Morley, C. K., Charusiri, P. and Watkinson, I. M., 2011, The geology of Thailand, Bath: The Geological Society of London: p. 626.

Morley, C. K., Ionnikoff, Y., Pinyochom, N., and Seusutthiya, K., 2007, Degradation of a footwall fault block with hanging-wall fault propagation in a continental-lacustrine setting: How a new structural model impacted field development plans, the Sirikit field, Thailand, AAPG Bulletin, V. 91, p. 1637-1661.

Pinyo, K., 2010, Petroleum system of the Chum Saeng Formation, Phitsanulok Basin, Thailand, Unpublished MSc. Thesis, Department of Geology and Geological Engineering, Colorado School of Mines, p. 41-45, p. 54-66.

PTTEP, 2015, Core Plugs petrographic analyses, Thailand, Weatherford KSP Company Limited.

Spiro B., Gibson P.J., and Shaw H.F., 1992, Eogenetic siderites in lacustrine oil shales from Queensland, Australia, Chemical Geology 398, Elsevier Science Publishers B.V. , p.415-427.

Srodon, J, 1979, Precise identification of illite/smectite interstratifications by x-ray powder diffraction, Institute of Geology, Polish Academy of Sciences, Poland, V.28, p. 401-411.

University of Sargodha, Pakistan, 2007, Deltas by University of Sargodha, Pakistan, http://www.slideshare.net/ay_arain39/deltas-13107361

Tultaveewat R., 2015, Fundamental control of low permeability sandstone Reservoirs, Published MSc. Thesis, Department of Geology, Chulalongkorn Universiry, p. 7-20.

Wittkop C. , Teranes J., Lubenowa B., Dean, W. E., 2014, Carbon- and oxygen-stable isotopic signatures of methanogenesis, temperature, and water column stratification in Holocene siderite varves, Chemical Geology 398, Elsevier Science Publishers B.V. , p.153-166.